# Deciphering Geochemical Traits of Orogenic Lushan Geothermal field in Taiwan

Yi-Chia Lu[1.2.3], Sheng-Rong Song[4], Ting-Jui Song[5], Tsung-Ren Peng[6], Hsiao-Fen Lee[7], Li-Hung Lin[4], Mien-Min Chen[8]

[1] Graduate Institute of Applied Geology, National Central University, Taoyuan, Taiwan

[2] Department of Earth Sciences, National Central University, Taoyuan, Taiwan

[3] Carbon Storage and Geothermal Research Center, National Central University, Taoyuan, Taiwan

[4] Department of Geosciences, National Taiwan University, Taipei, Taiwan

[5] Fabulous Power Co. Limited, Taipei, Taiwan

[6] Department of Soil and Environmental Science, National Chung Hsing University, Taichung, Taiwan

[7] Earth Sciences and Geotechnical Engineering Division, National Center for Research on Earthquake Engineering, Taipei, Taiwan

[8] Geological Survey and Mining Management Agency, MOEA, New Taipei, Taiwan

yichialu@cc.ncu.edu.tw

**Keywords:** *Lushan geothermal field, helium isotopic ratios, chemical components, hydrogen and oxygen isotope composition*

## ABSTRACT

The Lushan Geothermal Field, located within Taiwan's metapelitic orogenic belt, is recognized for its high geothermal gradient, making it a promising site for geothermal power plant development. The Silica geothermometer estimates indicate reservoir temperatures of up to 137℃ in Chunyang, 153℃ in Milegu, 183℃ in Lushan/Truwan, and 151℃ in Mahebo. Despite the highest temperatures recorded in the Lushan/Truwan area, the risk of landslides suggests that future drilling should be concentrated in the Chunyang and Milegu areas.

Seasonal variations significantly influence the chemical composition of hot springs in the Lushan Geothermal Field. During the dry season, the waters are primarily $Na_2CO_3$-rich, whereas in the wet season, they shift to $Ca(HCO_3)_2$ or even $CaSO_4$. The $\delta D$ and $\delta^{18}O$ values exhibit a concentrated pattern during the dry season and a more dispersed pattern during the wet season. These isotopic values do not clearly distinguish between the different areas within the geothermal field, such as Chunyang, Milegu, Lushan/Truwan, Mahebo, and Jingying, and variability within the same area suggests possible differences in local water circulation systems. The similarity between the $\delta D$ values of hot spring water and those of local rivers and groundwater indicates that the geothermal waters are likely derived from heated shallow groundwater rather than deep circulation or recharge from higher elevations. The $R_A$ ratio of helium isotopes indicating a crustal source mixed with atmospheric components. Furthermore, the hot spring waters are either saturated or supersaturated with minerals, highlighting the potential for scaling issues that must be addressed in any future geothermal power plant development in the area.

## 1. INTRODUCTION

### 1.1 Development of orogenic Geothermal System in Taiwan

Most geothermal power plants worldwide are built in high-enthalpy regions associated with magmatic activity, such as active volcanoes, recent plutonism (< 3 Ma), or extensional tectonics (Moeck, 2014). However, in Taiwan, active volcanoes are either located in national parks (Tatun Volcano Groups) or on offshore islands (Turtle Island), where development is restricted. Because geothermal energy can provide baseload, the Taiwanese government, aiming for net-zero carbon emissions by 2050, has prioritized geothermal development as a key renewable energy initiative. The goal is to achieve 200 MW by 2030, with the potential to reach 2 GW by 2040 and 6 GW by 2050, assuming Enhanced Geothermal Systems (EGS) and Advanced Geothermal Systems (AGS) technologies become viable. Consequently, the metapelitic non-volcanic geothermal fields in the orogenic belt have drawn increased attention. This article presents the geochemical findings from the investigation report "Construction of Underground 3D Geological Model in the Lushan Field" commissioned by the Geological Survey and Mining Management Agency.

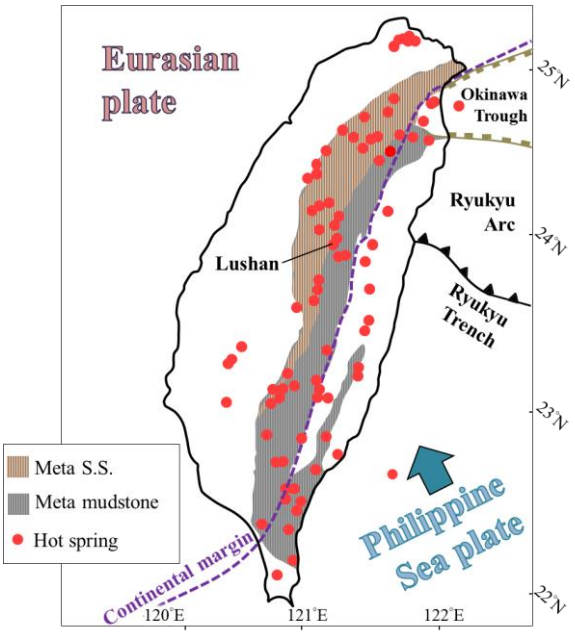


**Figure 1: Taiwan's geological setting and the location of Lushan geothermal field.**

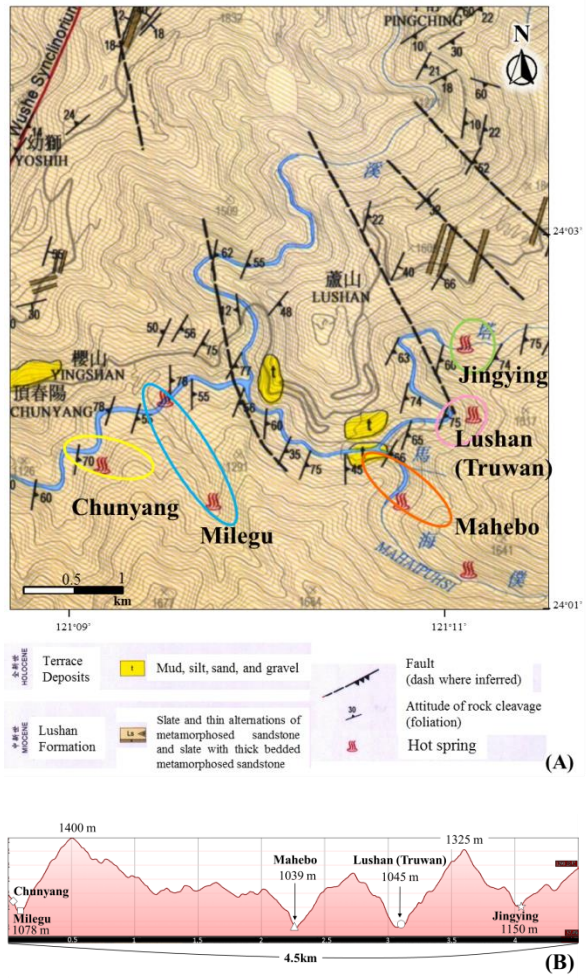


**Figure 2: (A) Geological map of the study area (Modified from Lo and Yang, 2002) (B) The elevations of the various hot spring areas within the Lushan Geothermal Field. (C) The Lushan Geothermal Field includes the Chunyang, Milegu, Lushan/Truwan, Mahebo, and Jingying.**

### 1.2 Geological Background

The geothermal potential in Taiwan's orogenic belt is largely attributed to its young orogenic activity. Around 5 million years ago, the Philippine Sea Plate began exerting a northwestward pressure on the Eurasian Plate at a rate of 4.9–8.5 cm/year (Hsu et al., 2016), leading to arc-continent collision (Byrne et al., 2011; Seno and Maruyama, 1984; Tsai et al., 1981; Yu and Chen, 1994). Throughout this process, the geological strata were compressed by approximately 150–200 km (Suppe, 1981). As a result, the sediments originally located on the continental shelf at the edge of the Eurasian continent were buried to depths of up to 10-12 kilometers withstand high temperatures of 250-350 ℃ (Chen and Wang, 1996) and were subsequently uplifted to the surface, forming mountains during the Late Pliocene (Chen and Wang, 1988b; Chen et al., 2019). This deep burial followed by uplift created a high geothermal gradient of up to 45 ℃/km, with localized heat flow reaching 140-250 mW/m² (Lee and Cheng, 1986; Chi and Reed, 2008). It is estimated that there are over 100 hot springs located at orogenic metapelitic region. The Lushan geothermal field is one of the most representative hot spring areas (Fig.1).

### 1.3 Geographical overview of Lushan Geothermal field

The Lushan Geothermal Field, situated in Nantou County, central Taiwan, encompasses an area of approximately 4.5 km², with elevations ranging from 1,039 to 1,150 m (Fig.2A and Fig.2B). This region is characterized by mountainous river valley topography, with pronounced fluvial downcutting and lateral erosion along both banks. The elevation difference between the streambed and the adjacent mountains can reach up to 440 m, resulting in the development of extensive landslide morphology. The regional geological structure of this area is primarily located east of Lishan Fault. The host rocks exhibit well-developed cleavage with a predominant NE-SW strike, dipping to the east at angles ranging 40-60 degrees. The folds are tightly compressed, and the strata are steeply inclined (Fig.2A).

The hot springs are primarily located along the banks of the upper Zhuoshui stream, and its sub-tributaries Truwan steam and Mahebo stream. The host rock in this region consists of meta-pelite interbedded with thin layers of fine-grained meta-sandstone (Fig.2A), with individual sandstone layers ranging from 5 to 20 cm in thickness, and occasionally reaching up to 10 m. The geological strata date back to the Early to Middle Miocene and are collectively referred to as the Lushan Formation, which is classified under the greenschist facies (Chen et al., 1983). The Lushan Geothermal Field features 5 primary hot spring outcrop areas: Chunyang Hot Spring Area, Milegu Hot Spring Stream, Lushan(Truwan) Hot Spring Stram, Mahebo Hot Spring Stream, and Jingying Hot Spring Area(Fig.2A and Fig.2C).

## 2. ANALYTICAL METHODS

### 2.1 Water sample analysis

In this study, 75 samples of hot spring water and well water (8 from the Chunyang, 15 from the Milegu, 29 from the Lushan/Truwan, and 16 from the Mahebo, and 7 from the Jingying) were collected from July 2022 to February 2024, with August 2023 experiencing a typhoon and landslides. During sampling, measurements were taken for temperature, pH, total dissolved solids (TDS), conductivity, salinity, and resistivity. The pH was measured using a Mettler-Toledo S2-Standard Kit paired with an InLab Expert Pro-ISM sensor, with a pH resolution of 0.01 and an accuracy of ±0.01. Conductivity was also measured using a Mettler-Toledo Cond portable S3-Standard Kit with an InLab 738-ISM sensor, which has a conductivity measurement range of



Proceedings 46th New Zealand Geothermal Workshop
20-22 November 2024
Auckland, New Zealand
ISSN 2703-4275

0.01 µS/cm to 500 mS/cm and an accuracy of ±0.5%, and is suitable for temperatures ranging from -5℃ to 105℃.

All samples were filtered through a 0.2 µm filter. After filtration, the liquid was used to rinse the filter funnel and sample bottles at least three times before collecting the filtrate. The liquid was stored in polypropylene bottles for the analysis of anions and titration of total alkalinity; concentrated hydrochloric acid was added to samples for the analysis of cations, and the liquid was stored in glass containers for the analysis of hydrogen and oxygen isotopes. Additionally, if necessary, pre-weighed deionized water was prepared to dilute the filtrate to 1/10 concentration for the analysis of silica content.

Water sample analyses were mainly conducted in the Department of Geosciences at National Taiwan University. This included analyzing silica and boron ions using Inductively Coupled Plasma Atomic Emission Spectroscopy (ICP-AES) made by Horiba, and analyzing major anions (fluoride, chloride, bromide, nitrate, phosphate, sulfate) and cations (lithium, sodium, ammonium, potassium, calcium, magnesium) in the hot spring water using 883 Intelligent Ion Chromatography made by Metrohm. Carbonate and bicarbonate concentrations in the hot spring were analyzed using the 877 Titrino Plus made by Metrohm, Switzerland. Hydrogen and oxygen isotope analyses were outsourced to the laboratory of the Department of Soil and Environmental Sciences at National Chung Hsing University, using a Liquid-Water Isotope Analyzer (LWIA).

### 2.2 Bubble gas analysis

Total of 6 bubble gas samples(3 from the Milegu, 2 from the Lushan/Truwan, and 1 from the Mahebo) were collected using the water displacement method, where bubbles from the hot spring pool were captured into pre-evacuated glass bottles. The compositions of gases were analysed using Gas Chromatography Mass Spectrometry made by Agilent in Taiwan Volcano Observatory of National Center for Research on Earthquake Engineering. The helium isotopic ratios were analysed by Micromass MM5400 in the Department of Geosciences at National Taiwan University.

## 3. RESULTS

In the Chunyang Hot Spring Area, the highest temperature data is from a 150m well, where the temperature can reach up to 79℃ after a period of discharge. The pH value ranges between 7.9 and 8.6, with total dissolved solids (TDS) and salinity reaching 1801 mg/L and 1.94 psu, respectively. In contrast, nearby surface hot springs have temperatures ranging from 36 to 46℃, pH values between 6.6 and 7.1, and TDS and salinity levels of only 500-1,058 mg/L and 0.53-1.15 psu. The Milegu Hot Spring Area has at least one boiling spring (92.1℃) with a pH value of 8.1, and TDS and salinity levels reaching 1681 mg/L and 1.81 psu, respectively. Due to the presence of hot spring outcrops along the entire stream, the water temperature throughout the stream is relatively high (>25℃). The temperatures of other hot spring outcrops range between the stream water and the boiling spring. Lushan/Truwan and Mahebo have similar conditions to Milegu, with boiling springs present in all areas, and numerous hot springs forming a hot spring river. During two years of sampling at Jingying, the highest measured hot spring temperature was 42.5°C, with a pH value of 6.7, and TDS and salinity levels reaching 468 mg/L and 0.50 psu, respectively.

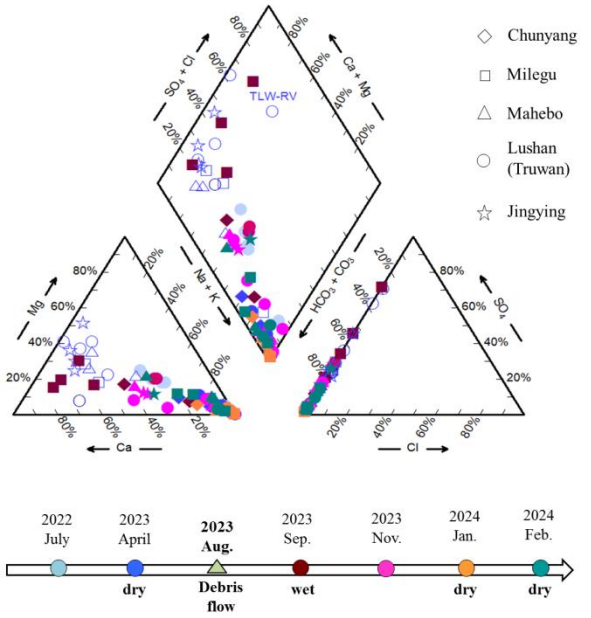


**Figure 3: When the major cation and anion compositions of the Lushan hot spring fluids are plotted on a Piper Diagram, a pronounced seasonal variation is observed. In the dry season, the waters are predominantly characterized by $Na_2CO_3$, whereas in the wet season, the composition shifts to $Ca(HCO_3)_2$ and $CaSO_4$. (Samples collected at different times are distinguished by color, with different symbols representing various sampling locations, and hollow symbols indicating river and groundwater samples.)**

The hot springs in the Lushan geothermal field (in cluding Chunyang, Milegu, Lushan/Truwan, Mahebo, or Jingying) primarily originate from deep pressurized aquifers, with $NaHCO_3$ as the main component. During the dry season, hot springs well up at the bottom of valleys, characterized by concentrated $\delta^{18}O$ values ranging from -9.2‰ to -8.9‰, and δD values ranging from -64.8‰ to -58.3‰. Higher cliffs emit steam. Consequently, during the wet season or following heavy rainfall, the rise in river water levels and groundwater leads some hot springs to transition to predominantly free groundwater compositions dominated by $Ca(HCO_3)_2$(Fig.3). This results in temperature reduction, pH decrease, Total Dissolved Solids (TDS) concentration decrease, and significant increases in $SO_4^{2-}$, $Mg^{2+}$, and $Ca^{2+}$ concentrations. δD and $\delta^{18}O$ values become more wide-ranging, with $\delta^{18}O$ values ranging from -10.7‰ to -7.3‰ and δD values ranging from -72.6‰ to -57.2‰ during the wet season, trending towards the meteoric water line(Fig.4). The significant alternation in ion composition between dry and wet seasons is a hallmark of the Lushan geothermal field.

Quartz geothermometers indicate that reservoir temperatures in the Chunyang, Milegu, Lushan/Truwan, and Mahebo can exceed and 137℃, 153℃, 183℃, and 151℃, respectively.



Proceedings 46th New Zealand Geothermal Workshop
20-22 November 2024
Auckland, New Zealand
ISSN 2703-4275

Hot spring bubble gas analysis reveals that $CO_2$ is the primary component in the Lushan area, constituting over 97%, followed by $N_2$ and $CH_4$(Table 1). The $R_A$ ratio of helium isotopes ranges from 0.35 to 1.00 (Table 2).

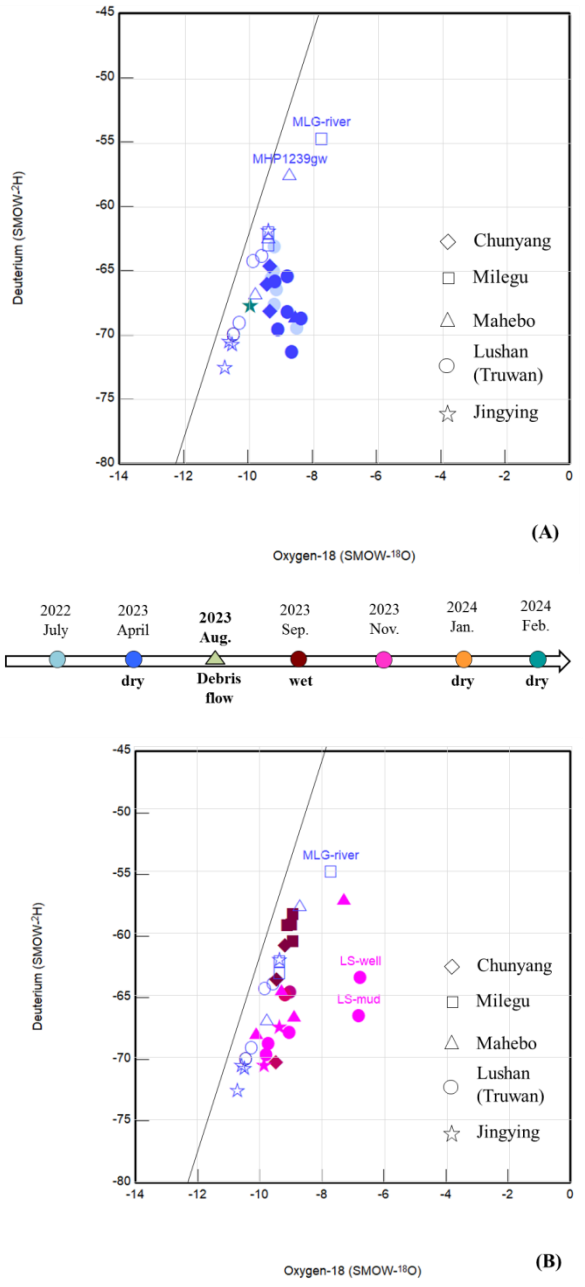


**Figure 4: Plots of hydrogen and oxygen isotopic values in (A) dry seasons and (B)wet seasons. (Samples collected at different times are distinguished by color, with different symbols representing various sampling locations, and hollow symbols indicating river and groundwater samples.) The Meteoric Water Line in Central Taiwan is referenced from $\delta^2H=8.1\ \delta^{18}O + 11.2$ (Peng et al., 2015).**

## 4. DISCUSSION

### 4.1 liquid and gas chemistry characteristics of Lushan

The Lushan geothermal field is located in an orogenic belt, where the heat source is attributed to a high geothermal gradient caused by rapid tectonic uplift, rather than magmatic activity or igneous intrusions. As a result, the fluid is primarily sodium bicarbonate, with a low chloride concentration (<15 mg/L). During the dry season, sulfate concentrations in hot spring well fluids are also low (<200 mg/L). However, in the wet season, sulfate concentrations in both stream and hot spring waters increase significantly, reaching up to 350 mg/L. This is likely due to the dissolution of pyrite, abundant in the surrounding slate, through oxidative weathering, releasing iron and sulfate ions.

Hydrogen and oxygen isotope analyses indicate that the water is of meteoric origin, with many samples closely aligned with the meteoric water line. In higher-temperature hot springs, a more significant $\delta^{18}O$-shift is observed, likely due to stronger water-rock interactions or boiling fractionation, or they may indicate deep metamorphic water contamination. Gas composition analyses show that $CO_2$ is the dominant gas, likely due to degassing during fluid ascent. The RA values, ranging from 0.35 to 1, suggest a mixture of atmospheric ($R_A$=1) and crustal ($R_A$=0.1) components, with no indication of mantle-derived input.

### 4.2 Geothermal development potential of Lushan

The results of the quartz geothermometer indicate that Lushan/Truwan has the highest geothermal potential in the region, with temperatures reaching up to 183℃. Drilling data from 1978 shows that well NL-1A recorded a temperature of 168℃ at just 227 m, and well NL-2 recorded 173℃ at 501 m, with a wellhead pressure of 11 kg/cm² and a flow rate of 33 tons/hr, demonstrating significant potential for geothermal power generation.

However, the 2023 typhoon triggered significant landslides, resulting in sediment accumulation nearly a story high in the riverbed, which buried numerous hot spring resorts in the vicinity. Additionally, access roads to Lushan/Truwan and Mahebo were severed. Long-term surface GPS monitoring has identified a deep-seated landslide risk on the adjacent Mu'an Mountain, which, if it were to occur, could devastate the entire area. In response, the government has designated this region as a hazardous zone and mandated the relocation of hot spring operators.

Given these safety concerns, any future geothermal development in this area is likely to focus exclusively on production wells. Consequently, this plan recommends that drilling exploration be directed toward areas with limited previous subsurface data, such as Chunyang and Milegu. While the projected reservoir temperatures in these locations may not match those of Lushan/Truwan and Mahebo, they present safer and more viable options for future geothermal development. In contrast, Jingying is deemed unsuitable for development due to significant dilution of spring water with stream water, making it impossible to accurately assess the reservoir temperature, and the area also lacks adequate land for development.

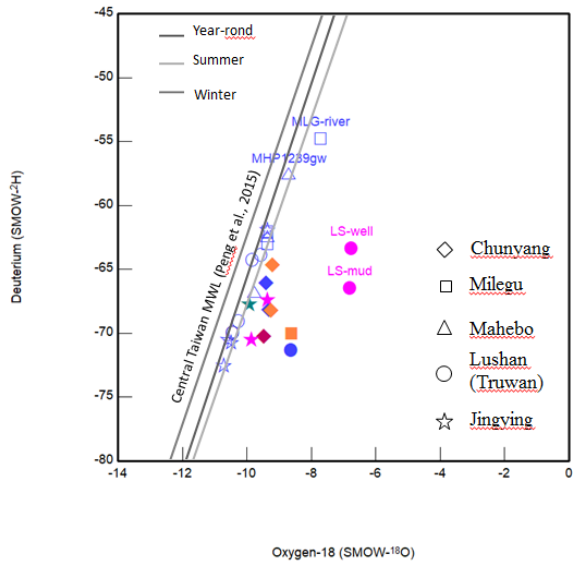


**Figure 5: Plots of hydrogen and oxygen isotopic values of well water and boiling springs.**

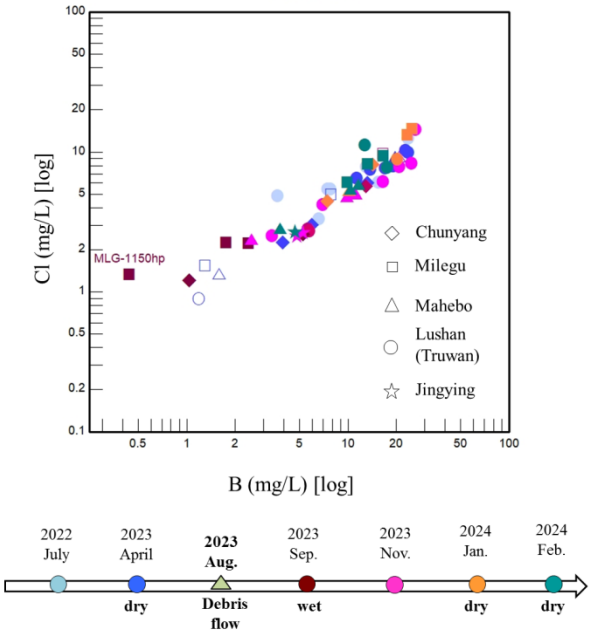


**Figure 6: Cl vs B binary diagram plot for hot springs from Lushan Geothermal field.**

### 4.3 Same/different reservoirs for five hot spring areas?

The Lushan Geothermal Field encompasses the southwestern regions of Chunyang and Milegu, as well as Lushan/Truwan, Mahebo, and Jingying to the northeast, spanning a straight-line distance of nearly 4 km and varying in elevation. However, when analyzing only the well water and boiling springs that most accurately represent reservoir fluids, hydrogen and oxygen isotope data do not reveal significant distinctions between these areas (Fig.5). The similarity in isotope values suggests that the original thermal fluids may have originated from comparable elevations.

In volcanic regions, the Cl/B ratio is commonly used to assess the relationships between hydrothermal systems in different areas. However, in the Lushan geothermal field, the chloride concentration in hot springs is less than 15 mg/L, and the boron concentration is less than 27 mg/L. Unlike hot springs in volcanic regions, where significant differences in chloride and boron concentrations are observed, plotting these two elements (Fig. 6) does not clearly distinguish the hot springs in different areas. Instead, the data are more noticeably influenced by seasonal variations, such as dry and wet seasons.

As a result, geochemical data alone is insufficient to conclusively determine whether these hot spring areas are fed by the same or distinct fluid sources. To ascertain the potential interconnections among these geothermal areas, it is imperative to incorporate additional geophysical data, such as Magnetotellurics (MT) and microseismicity, to provide a more comprehensive explanation.

### 4.4 Shallow groundwater circulation?

Historically, the hot springs within Taiwan's orogenic belt have been interpreted through the High Mountain-Deep Valley theory (Chen, 1982). This theory posits that precipitation, originating from moisture intercepted by high mountains, infiltrates through the groundwater system to considerable depths, where it is heated by the geothermal gradient. The heated water then ascends to the surface via fault or fracture systems. Consequently, in prominent geothermal fields such as Chingshui and Tuchang-Jentse, δD values in hot spring waters are significantly lighter than those of local meteoric water, while $\delta^{18}O$ values are elevated due to an oxygen shift resulting from water-rock interactions.

However, in the Lushan Geothermal Field, despite the occurrence of an oxygen shift, the δD values closely resemble those of local stream water and groundwater. Helium isotope analysis further reveals that the hot spring gases in this area are a mixture of crustal and atmospheric components. These observations lead us to hypothesize that the hydrothermal fluids in the Lushan Geothermal Field are rapidly heated at shallow depths following infiltration, likely due to the elevated temperatures of the surrounding rocks. This condition inhibits the extensive deep infiltration of meteoric fluids, resulting in the frequent discovery of high-temperature hot water at shallow depths. Although temperature increases with depth, deeper formations predominantly exhibit characteristics of hot dry rock.

### 4.5 Scaling potential

Due to the high bicarbonate content in the hot spring and well fluids of the Lushan Geothermal Field, calculations of the saturation index indicate that most fluids in the area are either oversaturated or nearly saturated with carbonate minerals. Additionally, as geothermal water ascends, the pressure decreases, causing dissolved $CO_2$ to escape, which further drives the reaction equilibrium towards precipitation. As a result, travertine deposits are commonly found at outcrops in the Lushan Geothermal Field, and calcite or aragonite precipitates are frequently observed at wellheads or on pipe walls. If a geothermal power plant is to be constructed in the Lushan Geothermal Field in the future, carbonate scaling will be a critical issue that must be addressed.

## 5. CONCLUSION

The hot springs in the Lushan geothermal field exhibit different chemical characteristics during the dry and wet seasons. During the dry season, they are primarily composed of $Na_2CO_3$, while during the wet season, they shift to $Ca(HCO_3)_2$ or even $CaSO_4$. The δD and $\delta^{18}O$ values are concentrated during the dry season and dispersed during the wet season.

The δD and $\delta^{18}O$ values cannot distinguish between Chunyang, Milegu, Lushan/Truwan, Mahebo, and Jingying. Isotopic values within the same area also show dispersion, indicating potential differences in water circulation systems within the same region. The δD values of the hot spring water are similar to those of the local river and groundwater, suggesting that these waters are likely heated shallow groundwater from nearby areas rather than being recharged from higher mountainous regions or undergoing deep circulation.

The reservoir temperatures estimated by the silica geothermometer for Chunyang are up to 137℃, Milegu are up to 153℃, for Lushan/Truwan 183℃, and for Mahebo 151 ℃. Although the Lushan/Truwan area appears to have the highest temperatures, considering the risk of landslides, future drilling is recommended in the Chunyang and Milegu areas, where subsurface data is currently limited.

The hot spring waters in the Lushan geothermal field are either saturated or supersaturated, indicating potential scaling issues for future geothermal power plant development.

## ACKNOWLEDGEMENTS

This work was supported by the Geological Survey and Mining Management Agency under the project "Construction of an Underground 3D Geological Model in the Lushan Field." The funding for attending the New Zealand Geothermal Workshop was provided by the National Science and Technology Council [NSTC 111-2116-M-008-022-MY3].

## REFERENCES

Byrne, T., Chan, Y.C., Rau, R.J., Lu, C.Y., Lee,Y.H., Wang, Y.J., 2011. The Arc–Continent Collision in Taiwan, in Arc-Continent Collision, D. Brown, P. D. Ryan, Eds. Springer Berlin Heidelberg, Berlin, Heidelberg, 213–245.

Chen, C.S., 1982. A Simple Geological Model for Geothermal Systems In The Central Range of Taiwan. Trans. 3rd Circum-Pacific Energy Miner. Resour. Conf. 393–397.

Chen, C.H., 1983. Analysis of topographic effect on ascending thermal water in the Central Range of Taiwan. Proc. Natl. Sci. Counc., Part A, 6: 241–249.

Chen, C.T., Chan, Y.C., Beyssac, O., Lu, C.Y., Chen, Y.G., Malavieille, J., Kidder, S.B., Sun, H.C., 2019. Thermal history of the northern taiwanese slate belt and implications for wedge growth during the neogene arc-continent collision. Tectonics 38 (9), 3335–3350.

Chen, W.S., Wang, Y., 1988b. The Plio-Pleistocene Basin Development In The Coastal Range Of Taiwan. Symposium on the Arc-Continent Collision and Orogenic Sedimentation in Eastern Taiwan and Ancient Analogs, Handbook, Taiwan, ROC, pp.21–22. (Chinese content)

Chen, W.S., Wang, Y., 1996. Geology of the eastern coastal mountains of Taiwan. Central Geological Survey, Ministry of Economic Affairs, 101 p.p. (Chinese content)

Chi, W.C. and Reed, D.L., 2008. Evolution of shallow, crustal thermal structure from subduction to collision: An example from Taiwan: Geological Society of America Bulletin, vol. 120, p. 679–690.

Hsu,W. H., Byrne,T. B., Ouimet, W., Lee,Y. H., Chen,Y. G., Soest, M. van, Hodges, K., 2016. Pleistocene onset of rapid, punctuated exhumation in the eastern Central Range of the Taiwan orogenic belt. Geology 44, 719–722.

Lee, C.R. and Cheng, W.T., 1986. Preliminary heat flow measurements in Taiwan, in 32 Western Pacific Earth Sciences, Vol.13.

Lo, W. and Yang, C.N., 2002. Wushe - Geological map of Taiwan scale 1:50,000. Geological Survey and Mining Management Agency. 26.

Moeck, I., 2014. Catalog of geothermal play types based on geologic controls. Renewable and Sustainable Energy Reviews, 37, 867–882.

Peng, T.R., Chen, K.Y., Zhan, W.J. Lu, W.C., Tong, L.T. , 2015. Use of stable water isotopes to identify hydrological processes of meteoric water in montane catchments. Hydrol Process. 29, 23, 4957–4967.

Seno, T., Maruyama, S., 1984. Paleogeographic reconstructionand origin of the Philippine sea. Tectonophysics 102, 53–84.

Suppe, J., 1981. Mechanics of Mountain Building and Metamorphism in Taiwan. Memoir of the Geological Society of China, No. 4, 67-89.Fournier, R.O., Potter, R.W.: Revised and expanded silica (quartz) geothermometer. Geotherm. Res. Council Bull. 11, 3–12.

Tsai, Y.B., Liaw, Z.S., Lee, T.Q., Lin, M.T., Yeh, Z.H., 1981. Seismological evidence of an active plate boundary in the Taiwan area. Mem. Geol. Sot. China 4, 143–154.

Yu, S.B., Chen, H.Y., 1994. Global Positioning System measurements of crystal deformation in the Taiwan arc-continent collision zone. Terr. Atom. Ocean. 5, 477–498.

**Table 1: Gas analysis result.**

| Before removing water | | | | | | | | | | | |
|---|---|---|---|---|---|---|---|---|---|---|---|
| Sample Name | Ar | $N_2$ | CO | $CH_4$ | He | $H_2$ | $O_2$ | $S_{total}$ | HCl | $CO_2$ | $H_2O$ |
| MLG 1137 | 3.21 | 132 | b.d.l. | b.d.l. | b.d.l. | 0.26 | 62.1 | 3.63 | 9.44 | 13087 | 986702 |
| MLG 1336 | 2.91 | 89 | b.d.l. | b.d.l. | b.d.l. | 1.05 | 48.3 | 10.5 | 23.6 | 17278 | 982547 |
| LS 1315 | 26.7 | 819 | b.d.l. | 152 | 0.58 | 1.50 | 377 | 37.0 | 87.6 | 91607 | 906891 |
| LS 1407 | 77.6 | 2311 | b.d.l. | 774 | 0.00 | 79.0 | 1597 | 89.0 | 368 | 399232 | 595473 |
| MHP 1203 | 10.0 | 547 | b.d.l. | 85.6 | 0.16 | 0.50 | 206 | 21.3 | 37.9 | 31475 | 967617 |
| MLG 1103 | 39.1 | 1324 | b.d.l. | 5406.6 | 3.75 | b.d.l. | 2.47 | 3.11 | 249 | 369 | 289 |
| After removing water | | | | | | | | | | | |
| Sample Name | Ar | $N_2$ | CO | $CH_4$ | He | $H_2$ | $O_2$ | $S_{total}$ | HCl | $CO_2$ | |
| MLG 1137 | 241 | 9932 | b.d.l. | b.d.l. | 0.00 | 19.5 | 4670 | 273 | 710 | 984155 | |
| MLG 1336 | 167 | 5076 | b.d.l. | b.d.l. | 0.00 | 60.1 | 2770 | 599 | 1355 | 989973 | |
| LS 1315 | 287 | 8795 | b.d.l. | 1637 | 6.19 | 16.1 | 4050 | 397 | 940 | 983870 | |
| LS 1407 | 192 | 5712 | b.d.l. | 1913 | 0.0 | 195 | 3947 | 220 | 910 | 986912 | |
| MHP 1203 | 310 | 16884 | b.d.l. | 2644 | 4.98 | 15.4 | 6349 | 657 | 1172 | 971965 | |
| MLG 1103 | 53.0 | 1797 | b.d.l. | 7338 | 3.35 | 4.21 | 337 | 501 | 337 | 989568 | |

μmol/

**Table 2: Helium isotope analysis result.**

| Sample name | $^4He/^{20}Ne$ | $^3He/^4He$ | $R_A$ | error (%) | [He]ppm |
|---|---|---|---|---|---|
| LS-1407 | 0.443 | 1.38405E-06 | 1.00 | 1.87 | 0.94 |
| LS-1315 | 0.702 | 8.74611E-07 | 0.63 | 1.70 | 1.13 |
| MLG-1137 | 0.318 | 1.36384E-06 | 0.98 | 0.83 | 5.37 |
| MLG-1336 | 0.805 | 7.68854E-07 | 0.55 | 1.45 | 1.13 |
| MLG-1103 | 2.832 | 4.81665E-07 | 0.35 | 1.84 | 0.56 |
| MHP-1203 | 1.999 | 7.53857E-07 | 0.54 | 1.57 | 1.25 |


ISSN 2703-4275